ARTICLE

doi:10.1016/j.ymthe.2005.06.001

Amelioration of both Functional and Morphological Abnormalities in the Retina of a Mouse Model of Ocular Albinism Following AAV-Mediated Gene Transfer

Enrico Maria Surace,[1] Luciano Domenici,[2,3] Katia Cortese,[4] Gabriella Cotugno,[1] Umberto Di Vicino,[1] Consuelo Venturi,[4] Alessandro Cellerino,[2,5] Valeria Marigo,[1] Carlo Tacchetti,[4] Andrea Ballabio,[1] and Alberto Auricchio[1,*]

[1]*Telethon Institute of Genetics and Medicine, Via P. Castellino 111, Naples 80131, Italy*
[2]*Istituto di Neuroscienze del CNR, Pisa 56100, Italy*
[3]*International School for Advanced Studies, Cognitive Neuroscience Sector, Trieste 34014, Italy*
[4]*MicroSCoBiO Research Center and IFOM Center of Cell Oncology and Ultrastructure, Department of Experimental Medicine, University of Genova, 16132 Genoa, Italy*
[5]*Scuola Normale Superiore, Pisa 56100, Italy*

**To whom correspondence and reprint requests should be addressed. Fax: +39 081 6132351. E-mail: auricchio@tigem.it.*

Available online 14 July 2005

X-linked recessive ocular albinism type I (OA1) is due to mutations in the *OA1* gene (approved gene symbol *GPR143*), which is expressed in the retinal pigment epithelium (RPE). The *Oa1* (*Gpr143*) knockout mouse (*Oa1*$^{-/-}$) model recapitulates many of the OA1 retinal morphological anomalies, including a lower number of melanosomes of increased size in the RPE. The *Oa1*$^{-/-}$ mouse also displays some of the retinal developmental abnormalities observed in albino patients such as misrouting of the optic tracts. Here, we show that these anomalies are associated with retinal electrophysiological abnormalities, including significant decrease in a- and b-wave amplitude and delayed recovery of b-wave amplitude from photoreceptor desensitization following bright light exposure. This suggests that lack of Oa1 in the RPE impacts on photoreceptor activity. More interestingly, adeno-associated viral vector-mediated *Oa1* gene transfer to the retina of the *Oa1*$^{-/-}$ mouse model results in significant recovery of its retinal functional abnormalities. In addition, *Oa1* retinal gene transfer increases the number of melanosomes in the *Oa1*$^{-/-}$ mouse RPE. Our data show that gene transfer to the adult retina unexpectedly rescues both functional and morphological abnormalities in a retinal developmental disorder, opening novel potential therapeutic perspectives for this and other forms of albinism.

Key Words: ocular albinism, retina, AAV, rescue of retinal function

INTRODUCTION

Congenital hypopigmentary diseases ("albinism") result from a defect in the synthesis or distribution of melanin pigment [1]. Melanin is responsible for skin, hair, and eye pigmentation. It is synthesized from the amino acid tyrosine in special organelles, the melanosomes. Different forms of albinism are due to mutations in genes involved in melanin production and accumulation [2]. Ocular albinism (OA) affects primarily the eye; oculocutaneous albinism (OCA) affects the skin and hair in addition [1].

Ocular albinism type I (OA1; MIM 300500) is the most common OA form [1]. OA1 is transmitted as an X-linked trait, with affected males showing the complete phenotype and heterozygous carrier females showing only minor signs of the disease. Visual abnormalities in OA1 are similar to those present in all forms of albinism [1,3]. OA1 male patients have reduced visual acuity, which represents a major handicap; nystagmus; strabismus; and marked photophobia [1]. This results from a developmental disorder of the retina characterized by foveal hypoplasia and misrouting of the optic fibers at the chiasm [3]. In addition, unlike other forms of albinism, the OA1 retinal pigment epithelium (RPE) and, to a lesser extent, the skin melanocytes present with characteristic large pigment granules, the macromelanosomes, suggesting that abnormal melanosomal biogenesis might occur in OA1 [4–6].

The gene responsible for OA1 (*OA1*; approved gene symbol *GPR143*), located in Xp22.3, has been identified

1525-0016/$30.00

by positional cloning [7]. It encodes an orphan G-protein-coupled receptor, which crosses the melanosomal membrane. Oa1 is expressed exclusively in RPE and skin melanocytes [8–12] and its transcript is detectable in murine embryonic RPE from early stages of development [10]. A mouse knockout (KO) model, which shows some of the OA1 landmarks, has been generated [13]. The *Oa1* −/y male or −/− female mice (referred to as *Oa1*$^{-/-}$ mice in this article) are viable and fertile. Ophthalmologic examination shows hypopigmentation of the ocular fundus in mutant animals compared with wild type [13]. Microscopic examination of the RPE shows the presence of macromelanosomes already detectable at birth (P1) and comparable with those described in OA1 patients [13]. In addition, *Oa1*$^{-/-}$ mice (similar to the OA1 patients) show abnormal crossing of the optic fibers at the chiasm, which occurs between embryonic days 12 and 18 in mice [13–15]. Foveal hypoplasia cannot be evaluated in rodents, who lack this structure. The *Oa1* mouse KO represents a unique model for the elucidation of the OA pathophysiology and for testing potential therapies for an otherwise untreatable ocular disorder. Gene transfer holds great promise for the treatment of inherited retinal diseases [16,17]. Vectors based on adeno-associated viruses (AAV) are able to transduce the retina of animal models of retinal diseases stably and efficiently and their toxicity and efficacy will be soon evaluated in the human retina [18–20]. We and others have shown that AAV vectors with an AAV1 capsid (AAV2/1) efficiently transduce the murine RPE [21–23], thus representing important tools for the treatment of animal models of RPE defects, such as the *Oa1*$^{-/-}$ mouse.

Retinal electrophysiological function has been analyzed in albino (OCA) rodents and abnormalities in both

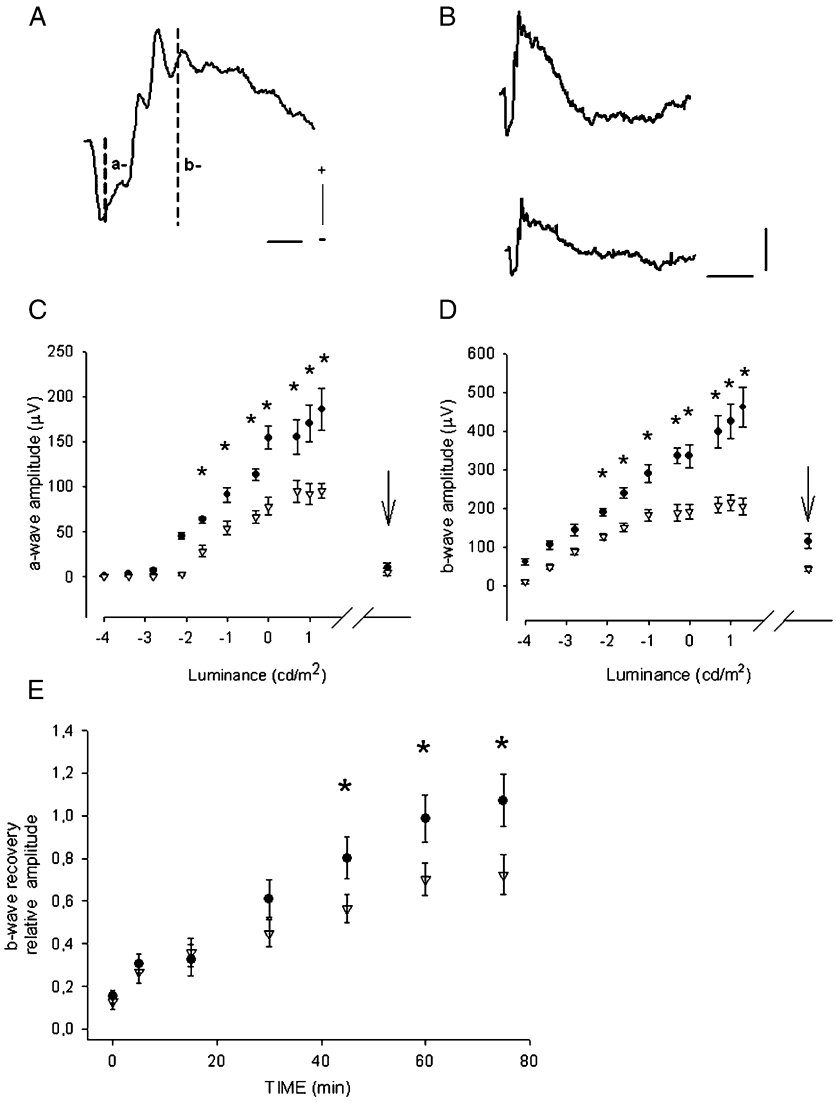

FIG. 1. Electrophysiological abnormalities in *Oa1* mice. ERGs were recorded after dark adaptation. (A) Typical ERG produced by a flash (10 cd m^{-2}) in a dark-adapted wild-type C57BL/6 mouse: a- and b-waves are indicated in an expanded scale (horizontal bar, 20 ms; vertical bar, 150 μV). Dotted lines refer to a- and b-wave amplitudes. (B) ERG produced by a flash (1 cd m^{-2}) in a wild-type C57BL/6 (upper waveform) and an *Oa1*$^{-/-}$ (lower waveform) mouse; horizontal bar, 100 ms; vertical bar, 200 μV. ERG components under scotopic and photopic conditions: (C) a- and (D) b-waves in *Oa1*$^{-/-}$ and C57BL/6 wild-type mice. The amplitudes (mean ± SEM) evoked by increasing light intensities under scotopic conditions in *Oa1*$^{-/-}$ mice (empty triangles, n = 10 eyes) and age-matched controls (black circles, n = 10 eyes) are shown. The amplitude of a- and b-waves elicited under photopic conditions is indicated by an arrow. (E) Recovery of b-wave amplitude after bleaching condition (600 cd m^{-2} for 3 min) in *Oa1*$^{-/-}$ (empty triangles, n = 12 eyes) and wild-type C57BL/6 mice (black circles, n = 12 eyes). The amplitude of b-wave after bleaching condition was measured for flash of 1 cd m^{-2} s^{-1} and expressed as relative mean value compared to the amplitude of b-wave measured before bleaching condition. Asterisks depict statistical significance ($P < 0.05$).

doi:10.1016/j.ymthe.2005.06.001

TABLE 1: Values of mean b-wave amplitudes—including standard deviation and error—at different time points before (–4 min) and after photoreceptor desensitization

C57BL/6				C57BL/6 *Oa1*$^{-/-}$		
Mean b-wave (μV)	Standard deviation	Standard error	Time (min)	Mean b-wave (μV)	Standard deviation	Standard error
201.3201	72.16918313	22.82189956	–4	119.3180833	58.16576671	16.79101053
24.7725	16.57714234	5.242152688	0	12.79395	7.750638312	2.450967039
48.0427	26.40620808	8.350376191	5	27.2946	15.88910123	5.024574985
70.2866	69.77704883	22.06544027	15	37.4196	27.44337372	8.678356765
115.6165	95.11824733	30.07903086	30	49.0226	31.59256886	9.990447472
138.601	83.33688361	26.35343653	45	62.1566	34.21601797	10.82005493
180.1548	87.90791193	27.7989226	60	75.6743	43.81319146	13.85494766
191.8519	88.42408257	27.96215009	75	80.1195	31.17113631	12.72556311

light-evoked responses and ability to recover from photoreceptor desensitization following bright light exposure (dark adaptation) have been described [24–27]. Here we report for the first time the identification of electrophysiological abnormalities of the *Oa1*$^{-/-}$ mouse retina and the demonstration that delivery of the *Oa1* gene with AAV vectors to the *Oa1*$^{-/-}$ mouse adult retina significantly rescues these electrophysiological abnormalities as well as the RPE melanosomal defects. This suggests that at least some of the retinal functional and ultrastructural defects in a developmental disorder of the retina can be rescued by gene transfer, which, therefore, represents a potential therapeutic strategy for OA1 and other forms of albinism.

RESULTS AND DISCUSSION

Abnormal Electrophysiological Activity of the *Oa1* Knockout Retina

To test whether *Oa1* gene knockout results in abnormal retinal function, we performed extensive electrophysiological analysis in *Oa1*$^{-/-}$ and wild-type, age-matched C57BL/6 mice. We measured Ganzfeld flash electroretinograms (ERG) after 3 h dark adaptation in *Oa1*$^{-/-}$ and wild-type mice (8–9 months of age, Fig. 1). The amplitude of ERG a- (Figs. 1B and 1C) and b- (Figs. 1B and 1D) waves is significantly decreased in *Oa1*$^{-/-}$ mice compared to wild-type C57BL/6 mice, suggesting abnormal photoreceptor function as a result of absence of the *Oa1* gene. Compared to the scotopic responses, photopic ERG was affected to a lesser extent (statistical significance among the *Oa1*$^{-/-}$ and wild-type animals was not reached using the ANOVA test described under Material and Methods), suggesting that absence of Oa1 impairs mainly the rod pathway. A similar shift toward lower intensities has been recently observed in other albino mice [24,25,27]. These combined results suggest that the RPE defect in albinism, whether due to absence of melanin or to abnormal melanosomal biogenesis, impacts on photoreceptor function as assessed by flash ERG analysis.

We then analyzed the ability of the *Oa1*$^{-/-}$ mouse retina to recover from a photoreceptor-desensitizing light stimulus (dark adapt), which has been reported to be delayed in rodents affected by different types of albinism [25–27]. We exposed the mice to an intense bleaching condition (600 cd m^{-2} for 3 min) before monitoring the recovery of b-wave using a flash of 1 cd m^{-2} s^{-1}. We measured recovery of b-wave amplitude over

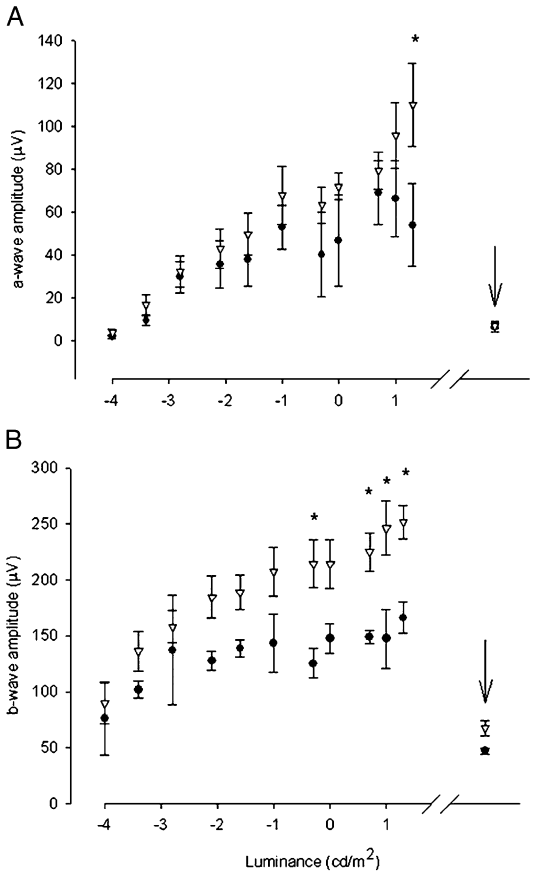

FIG. 2. Partial recovery of the rod function following subretinal delivery of AAV2/1-CMV-m*Oa1* to *Oa1*$^{-/-}$ mice. Amplitude of (A) a- and (B) b-waves under scotopic and photopic (depicted by the arrows) conditions (mean ± SEM) from AAV2/1-CMV-m*Oa1*- (empty triangles, $n = 5$) and AAV2/1-CMV-*EGFP*- (black circles, $n = 3$) treated eyes recorded 1 month after vector delivery. Asterisks depict statistical significance ($P < 0.05$).

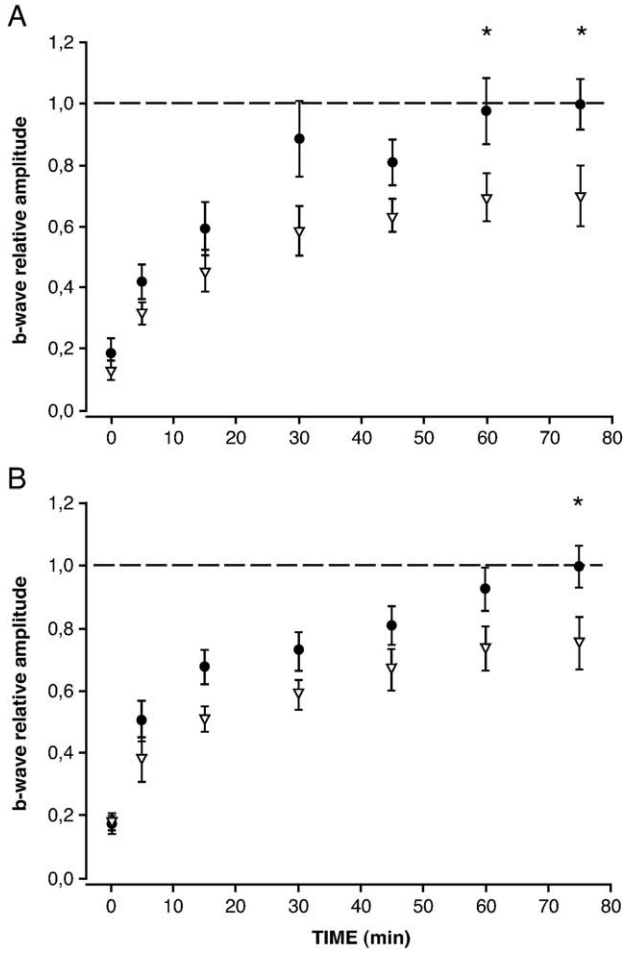

FIG. 3. Rescue from delayed recovery from photoreceptor desensitization in *Oa1*$^{-/-}$ mice treated with AAV. Progressive recovery over time of the b-wave amplitude following bleaching conditions in (A) 2- and (B) 9-month-old *Oa1*$^{-/-}$ animals injected subretinally with either AAV2/1-CMV-m*Oa1* (black circles, $n = 6$ eyes in both A and B) or AAV2/1-CMV-*EGFP* (empty triangles, $n = 6$ eyes in A and 9 in B). Asterisks depict statistical significance ($P < 0.05$).

time; the amplitude of the b-wave relative to that prior to photoreceptor desensitization is represented in Fig. 1E, while absolute values are depicted in Table 1. A significant delay in recovery from photoreceptor desensitization was observed in *Oa1*$^{-/-}$ mice compared to wild-type mice. The *Oa1*$^{-/-}$ mice b-wave did not recover 90 min after bleaching conditions, suggesting that prolonged functional uncoupling between the RPE and the photoreceptors may be a consequence of the absence of Oa1. Whether this is due primarily to the Oa1 pigment defect or to a secondary deficiency in the visual cascade (i.e., pigment regeneration) remains to be assessed.

Rescue of the Abnormal Electrophysiological Activity of the *Oa1*$^{-/-}$ Mouse Retina Following Gene Transfer

The finding of functional and ultrastructural *Oa1*$^{-/-}$ mouse retinal defects allows us to investigate whether these aspects of the *Oa1*$^{-/-}$ mouse phenotype might be reversible. This is relevant for the understanding of some crucial processes such as melanosome biogenesis and turnover and to evaluate the feasibility of therapies for a disease whose symptoms are already present at birth. For this purpose, we produced an AAV2/1 vector expressing the murine *Oa1* coding sequence under the control of the ubiquitous cytomegalovirus (CMV) promoter (AAV2/1-CMV-m*Oa1*) and we injected it subretinally into 1-month-old *Oa1*$^{-/-}$ mice. Four weeks later we analyzed Oa1 expression in retinal sections by immunofluorescence: a strong signal was detected in both RPE and photoreceptors (data not shown).

To test whether the *Oa1*$^{-/-}$ mouse photoreceptor dysfunction is reversible, we injected *Oa1*$^{-/-}$ mice (8 months of age) subretinally in one eye with 2–3 $\times$ 10^9 genome copies (GC) of a 1:1 mixture of AAV2/1-CMV-m*Oa1* + AAV2/1-CMV-*EGFP* (expressing the enhanced green fluorescence protein, EGFP) and in the contralateral eye with the same dose of AAV2/1-CMV-*EGFP* alone as control. Four weeks after vector administration, we performed indirect ophthalmoscopic evaluation to assess EGFP expression [21] followed by flash ERG analysis (Fig. 2). The b-wave amplitude elicited under photopic conditions was higher (albeit not statistically

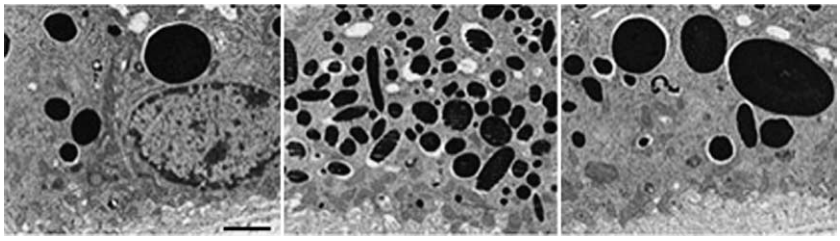

FIG. 4. Increased density of normal-sized stage IV melanosomes in the Oa1 retinae transduced with AAV. Representative electron micrographs of peripheral RPE in 2-month-old treated and control *Oa1*$^{-/-}$ retinae. Left shows the low melanosome density and macromelanosome presence typical of the *Oa1*$^{-/-}$ RPE transduced with AAV2/1-CMV-*EGFP*. Middle and right show different areas of the same RPE cell in a retina transduced with AAV2/1-CMV-m*Oa1*. Note the increased number of normal-sized melanosomes (middle) with persistence of macromelanosomes (right). Size bar, 1.5 μm.

doi:10.1016/j.ymthe.2005.06.001

significant) in *Oa1*-treated than in untreated mice, suggesting a partial rescue of cone function. In addition, both a- and b-wave amplitudes under scotopic conditions were significantly higher (albeit not normal) at the highest light intensities in the retinae injected with both the *Oa1* and the *EGFP* vector than in the contralateral eye injected with the vector expressing EGFP alone (Fig. 2).

These data suggest that a partial rescue of both rod and cone function occurred in the retinae expressing recombinant Oa1. Although AAV-mediated Oa1 expression was detected in both RPE and photoreceptors, the recovery of photoreceptor activity in the $Oa1^{-/-}$ mouse is likely due to robust transduction of the RPE, which is the only Oa1 physiological site of expression in the retina (and therefore affected in the KO animal). AAV-mediated Oa1 expression with RPE-specific promoters is being tested to rule out that Oa1 expression in photoreceptors might contribute to the partial rescue observed in photoreceptor function.

We then asked whether the delayed recovery from photoreceptor desensitization present in the $Oa1^{-/-}$ mice was reversible and whether this could be dependent on the age of the animals treated. For this purpose, we injected two cohorts of $Oa1^{-/-}$ mice of different ages (1 and 8 months) subretinally, similar to those presented in Fig. 2, and 4 weeks later tested their ability to adapt to dark (Fig. 3). Independent of the age of treatment, the retinae that received the *Oa1* vector completely recovered from the delay in dark adaptation in 75 min, similar to wild-type retinae. The contralateral *EGFP*-treated retinae do not recover after 90 min, the latest time point of the analysis in some animals. This suggests that *Oa1* gene delivery, applied at different time points to the adult retina, can rescue the delayed dark adaptation present in the mouse model. This could be relevant if gene delivery is considered for OA1 patients, as discussed below.

Modification of the *Oa1* RPE Ultrastructural Defects Following Gene Transfer

The modification in electrophysiological activity following gene transfer to the $Oa1^{-/-}$ mouse retina prompted us to investigate whether this could be related to changes occurring in the $Oa1^{-/-}$ RPE melanosomes, which are of lower number (V. Marigo *et al.,* unpublished results) and increased size from birth [13]. We enucleated eyes from some of the animals used for the experiment depicted in Fig. 3A. We dissected transduced, EGFP-positive areas from eyes injected either with the AAV2/1-CMV-m*Oa1* + AAV2/1-CMV-*EGFP* mixture or with the AAV2/1-CMV-*EGFP* vector alone under a fluorescence microscope. EGFP-positive, transduced areas accounted for 40–50% of the whole retina with minor interanimal variation (data not shown). We analyzed two different regions of the eye, one centrally located in the proximity of the optic nerve and the remaining peripheral region, representing the vast majority of the retina. We isolated the RPE from these regions and analyzed them by electron microscopy to assess melanosome number and size.

A representative picture from *Oa1*- or *EGFP*-injected eyes is shown in Fig. 4. In two independent electron microscopy measurements, the melanosome density

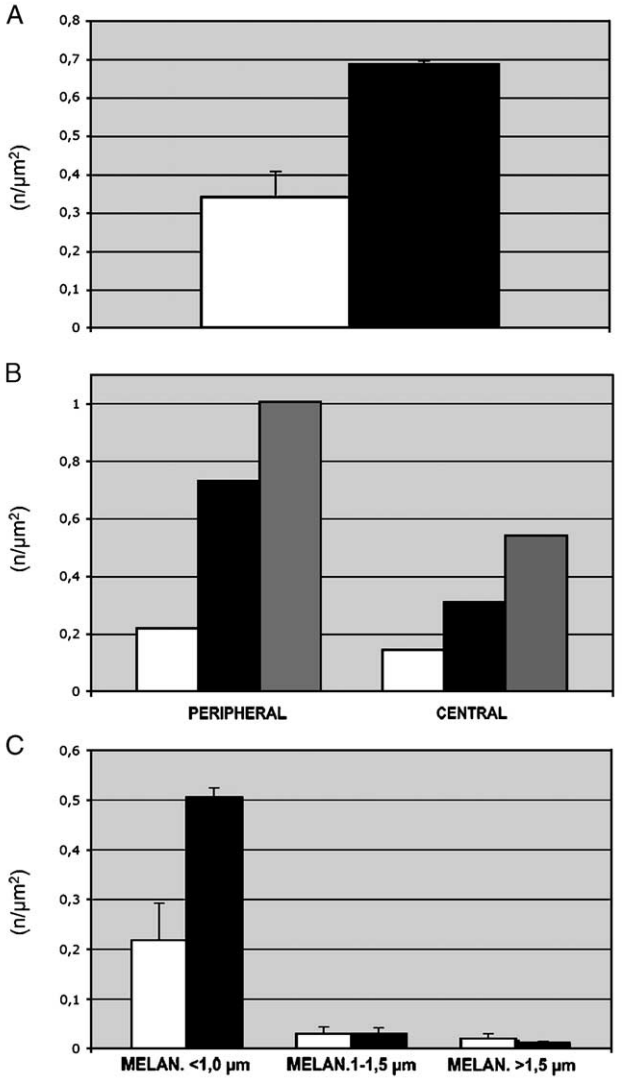

FIG. 5. Melanosomal modifications in the $Oa1^{-/-}$ RPE following delivery of AAV2/1-CMV-m*Oa1* (black bar) or AAV2/1-CMV-*EGFP* (white bar). (A) Mature (stage IV) melanosome density in the peripheral RPE (mean ± SEM; $n = 2$ eyes/group, two sections/eye). (B) Mature (stage IV) melanosomal density in the peripheral and central RPE area of AAV-treated and wild-type C57BL/6 (gray bar) retinae ($n = 1$ eye/group, mean of two sections/area). (C) Density of different-sized melanosomes in the peripheral RPE transduced with AAV (mean ± SEM; $n = 2$ eyes/group, two sections/eye). MELAN, melanosome size.

(melanosome/μm^2) in the peripheral RPE injected with the *Oa1*-expressing vector was higher than that measured in the same area of the contralateral eyes injected with the *EGFP* vector alone (Fig. 5A). In one eye, we analyzed both the transduced peripheral and central retinae, confirming that treatment with the *Oa1* vector increases melanosome density independent of the area of transduction (Fig. 5B). The number of normal-sized melanosomes in the peripheral RPE was increased in the two retinae treated with the *Oa1* vector compared to the contralateral eye treated with the *EGFP* vector alone, while the number of giant-size melanosomes (>1.5 μm) remained similar (Fig. 5C). This suggests that in the period following gene transfer (4 weeks) biogenesis of melanosomes of normal size occurs in the $Oa1^{-/-}$ RPE treated with the therapeutic vector rather than modification of the preexisting abnormal organelles.

In conclusion, we show that absence of the *Oa1* gene product in the RPE impacts on photoreceptor function in the $Oa1^{-/-}$ mouse model. How these electrophysiological abnormalities in mice reflect the defective visual function in OA1 patients remains to be determined. One could hypothesize that they might mirror photophobia and part of the decrease in visual acuity observed in the OA1 patients. We also show that gene transfer to the $Oa1^{-/-}$ mouse adult retina can rescue these electrophysiological abnormalities, as well as the altered melanosome density. Therefore, these results suggest that a reversible functional defect in the $Oa1^{-/-}$ retina exists, which can be recovered independent of the developmental abnormalities already irreversibly established at the time of gene transfer (i.e., misrouting of the optic fibers).

Given that albinism affects retinal development and that visual function is severely compromised but not lost in albino patients, it would not be considered a primary target for gene therapies. Nevertheless, the nonprogressive nature of the disease and the possibility of ameliorating visual function with treatment to the adult retina open novel therapeutic perspectives for albino patients.

Material and Methods

Generation of the pAAV2.1-CMV-Oa1 construct, AAV vector production, and purification. The murine *Oa1* coding sequence in pBS-SK plasmid was mutagenized via PCR using the Advantage cDNA PCR Kit (Clontech, Palo Alto, CA, USA) to eliminate the *Hin*dIII restriction site and to insert a *Not*I and a *Hin*dIII site at the 5′ and 3′ end, respectively, with the following primers: Oa1-NotI-F, AAGCGGCCGCATGGCCTCCCCGCGCCTGGGAATTTTCTGCTGCCCTACGTGGGACGCAGCCACACAGCTGGTGCTAAGTTTCCAAC, and Oa1-HindIII-R, TTGACTCCATTTCCCAAGCCCAGGGGGAACTCTGAAAGCTTAA. The PCR product was then digested with *Not*I and *Hin*dIII and cloned into pAAV2.1-CMV-EGFP [28] by removing the EGFP coding sequence (*Not*I–*Hin*dIII). AAV2/1-CMV-m*Oa1* and AAV2/1-CMV-*EGFP* vectors were produced by triple transfection, purified by $CsCl_2$ ultracentrifugation, and titered using a real-time PCR-based assay as previously described [21,28]. AAV vectors were produced by the AAV TIGEM Vector Core.

Subretinal vector administration. All procedures on mice (including their euthanasia) were performed in accordance with institutional guidelines for animal research. Oa1 (kept in a C57BL/6 background) and wild-type C57BL/6 mice were used (Charles River Italia, Lecco, Italy). For subretinal vector administration, mice were anesthetized with an intraperitoneal injection of avertin at 2 ml/100 g body wt (1.25% (w/v) 2,2,2-tribromoethanol and 2.5% (v/v) 2-methyl-2-butanol; Sigma–Aldrich, St. Louis, MO, USA) and viral vectors were delivered via a transscleral transchoroidal approach as described [29].

Immunofluorescence. One month after injection treated and control eyes were collected, fixed overnight in 4% paraformaldehyde, incubated in 30% sucrose for 2 h, and then frozen in OCT compound (Kaltech, Padua, Italy). Serial cryosections (12 μm thick) were obtained. To detect Oa1 by immunofluorescence, cryosections were fixed in 4% paraformaldehyde for 20 min, washed, and incubated at room temperature in 30 mM NH_4Cl for 30 min. Sections were then permeabilized and blocked against nonspecific binding in a buffer containing 10% FBS (GIBCO, Invitrogen Life Technologies, Carlsbad, CA, USA), 0.1% saponin in PBS overnight at 4°C. Samples were then washed with PBS and incubated with rabbit anti-mouse-Oa1 primary antibody (1:50 diluted in 0.01% saponin) for 2 h at room temperature. After extensive washing in 0.01% saponin, sections were incubated with secondary Cy2-labeled anti-rabbit antibody (Jackson ImmunoResearch, Cambridgeshire, UK; 1:100 diluted in 0.01% saponin) for 1 h at room temperature, washed with PBS, and mounted with Vectashield mounting medium (Vector Laboratories, Burlingame, CA, USA). Treated slides were then analyzed under the Axioplan 2 imaging fluorescence microscope (Carl Zeiss, Milan, Italy).

Electrophysiological recordings. Flash ERG was evoked by 10-ms flashes of light generated through a Ganzfeld stimulator (Lace, Pisa, Italy). The electrophysiological signals were recorded through gold-plated electrodes inserted under the lower eyelids in contact with the cornea previously anesthetized with ossibuprocaine (Novesine, Novartis Pharma, Switzerland). The electrode in each eye was referred to a needle electrode inserted subcutaneously at the level of corresponding frontal region. The different electrodes were connected to a two-channel amplifier.

After 180 min of dark adaptation, mice were anesthetized by an intraperitoneal injection of avertin (1.2% tribromoethanol and 2.4% amylene hydrate in distilled water; 2 ml/100 g body wt) and loosely mounted in a stereotaxic apparatus under dim red light with the body temperature maintained at 37.5°C. For recordings under dark-adapted conditions we adopted the following protocol: after dark adaptation ERG was recorded in response to flash of different light intensities, ranging from 1×10^{-4} to 20 cd m^{-2} s^{-1}. The time interval between each stimulus was 4–5 min. Amplitudes of a- and b-waves were plotted as a function of increasing light intensity. After completion of responses obtained under dark-adapted conditions the recording session continued with the aim to dissect the cone pathway mediating the light response. To this aim the ERG in response to light of 20 cd m^{-2} s^{-1} was recorded in the presence of constant light background set at 20 cd m^{-2}.

In a different group of mice scotopic ERG was recorded in response to light of 1 cd m^{-2} s^{-1}. For screening purposes 10 different responses were averaged with an interstimulus interval of 2–4 s. Mice were then exposed to a constant light, the intensity of which was set at 600 cd/m^2 for 3 min (preadapting light, bleaching condition). Recovery of b-wave was monitored at fixed intervals after preadapting light (0, 5, 15, 30, 45, 60, 75 min). The amplitude of b-wave in response to a flash of 1 cd m^{-2} $s^{-}1$ after the preadapting light was measured and expressed as a relative value with respect to that measured before the preadapting light.

Data were statistically analyzed using the Statistica (Statsoft, USA: two-way ANOVA using least significance difference test for pair-wise comparisons).

Ultrastructural analysis of the $Oa1^{-/-}$ retinal pigment epithelium. $Oa1^{-/-}$ eyes injected with AAV2/1-CMV-m*Oa1* + AVV2/1-*EGFP* (right eyes) and AAV2/1-CMV-*EGFP* (left eyes) were removed and fixed in 2.5%

doi:10.1016/j.ymthe.2005.06.001

glutaraldehyde (PolyScience, Inc., Eppelheim, Germany) in 0.1 M cacodylate buffer (Sigma–Aldrich). The injected portion of the retina was identified with a dissecting microscope equipped with epifluorescence illumination. The EGFP-positive region was dissected and processed for electron microscopy analysis, as described [30]. Briefly, the dissected tissue was fixed 2 h in 2.5% glutaraldehyde in 0.1 M cacodylate buffer, postfixed 2 h in 1% osmium tetroxide (Electron Microscopy Science, Hatfield, PA, USA) in 0.1 M cacodylate buffer, and *en bloc* stained 2 h with 1% uranyl acetate (Electron Microscopy Science), at room temperature. Samples were then dehydrated through a graded ethanol series and propylene oxide (TAAB Laboratories Equipment Ltd., Aldermaston, England) and embedded in Poly-Bed (PolyScience, Inc.) epoxy resin. Ultrathin sections were obtained from two different areas of the RPE (peripheral and central retina) in each sample. For each area two series of sections at 60 μm distance from each other were collected. Samples were analyzed with FEI Tecnai 12-G2 TEM and FEI AnalySYS software (FEI Co., Eindhoven, The Netherlands). We analyzed the RPE of 2-month-old mice. The analysis was performed on a total of ~800 μm^2 for each series of sections, calculated with the "closed polygon" option of the software. We determined the density of total stage IV melanosomes (number of melanosomes/μm^2) and the diameter of stage IV melanosomes, calculated along the major axis of the organelle. We measured the diameter of melanosomes completely enclosed in each micrograph.

ACKNOWLEDGMENTS

We thank Maria Vittoria Schiaffino for the rabbit anti-mouse Oa1 primary antibody. This work was performed with the following funding: TIGEM Grants P04 and C25 from the Telethon Foundation (to A.A.), a grant from the Ruth and Milton Steinbach fund (to A.A.), FIRB RBN E01AP77 from the Italian Ministry of the University and Scientific Research (to A.A.), a grant from the Istituto Superiore di Sanita' (Progetto "Malattie Rare", to A.A.), Grant 1R01EY015136-01 from the NEI (to A.B.), and a grant from the Italian Ministry of Agriculture (to A.B.). Electron microscopy studies have been performed at the Telethon Facility for EM, Genoa, Italy (Grant GTF03001 to C.T.) and using a grant from the Italian Ministry of the University and Scientific Research to C.T. The continuous support of the Vision of Children Foundation is also gratefully acknowledged.

RECEIVED FOR PUBLICATION MARCH 22, 2005; REVISED 24 MAY 2005; ACCEPTED JUNE 7, 2005.

REFERENCES

1. King, R. A., Hearing, V. J., Creel, D. J., and Oetting, W. S. (2001). *Albinism: The Metabolic and Molecular Bases of Inherited Disease*. McGraw–Hill, New York.
2. Oetting, W. S., and King, R. A. (1999). Molecular basis of albinism: mutations and polymorphisms of pigmentation genes associated with albinism. *Hum. Mutat.* **13:** 99–115.
3. Creel, D. J., Summers, C. G., and King, R. A. (1990). Visual anomalies associated with albinism. *Ophthalmic Paediatr. Genet.* **11:** 193–200.
4. O'Donnell, F. E., Jr., Hambrick, G. W., Jr., Green, W. R., Iliff, W. J., and Stone, D. L. (1976). X-linked ocular albinism: an oculocutaneous macromelanosomal disorder. *Arch. Ophthalmol.* **94:** 1883–1892.
5. Garner, A., and Jay, B. S. (1980). Macromelanosomes in X-linked ocular albinism. *Histopathology* **4:** 243–254.
6. Yoshiike, T., Manabe, M., Hayakawa, M., and Ogawa, H. (1985). Macromelanosomes in X-linked ocular albinism (XLOA). *Acta Dermatol. Venereol.* **65:** 66–69.
7. Bassi, M. T., *et al.* (1995). Cloning of the gene for ocular albinism type 1 from the distal short arm of the X chromosome. *Nat. Genet.* **10:** 13–19.
8. Schiaffino, M. V., *et al.* (1996). The ocular albinism type 1 gene product is a membrane glycoprotein localized to melanosomes. *Proc. Natl. Acad. Sci. USA* **93:** 9055–9060.
9. Schiaffino, M. V., *et al.* (1999). Ocular albinism: evidence for a defect in an intracellular signal transduction system. *Nat. Genet.* **23:** 108–112.
10. Surace, E. M., Angeletti, B., Ballabio, A., and Marigo, V. (2000). Expression pattern of the ocular albinism type 1 (Oa1) gene in the murine retinal pigment epithelium. *Invest. Ophthalmol. Visual Sci.* **41:** 4333–4337.
11. Shen, B., Samaraweera, P., Rosenberg, B., and Orlow, S. J. (2001). Ocular albinism type 1: more than meets the eye. *Pigment Cell Res.* **14:** 243–248.
12. Schiaffino, M. V., *et al.* (2002). Effective retrovirus-mediated gene transfer in normal and mutant human melanocytes. *Hum. Gene Ther.* **13:** 947–957.
13. Incerti, B., *et al.* (2000). Oa1 knock-out: new insights on the pathogenesis of ocular albinism type 1. *Hum. Mol. Genet.* **9:** 2781–2788.
14. Herrera, E., *et al.* (2003). Zic2 patterns binocular vision by specifying the uncrossed retinal projection. *Cell* **114:** 545–557.
15. Williams, S. E., Mason, C. A., and Herrera, E. (2004). The optic chiasm as a midline choice point. *Curr. Opin. Neurobiol.* **14:** 51–60.
16. Bessant, D. A., Ali, R. R., and Bhattacharya, S. S. (2001). Molecular genetics and prospects for therapy of the inherited retinal dystrophies. *Curr. Opin. Genet. Dev.* **11:** 307–316.
17. Bennett, J. (2000). Gene therapy for retinitis pigmentosa. *Curr. Opin. Mol. Ther.* **2:** 420–425.
18. Auricchio, A. (2003). Pseudotyped AAV vectors for constitutive and regulated gene expression in the eye. *Vision Res.* **43:** 913–918.
19. Surace, E. M., and Auricchio, A. (2003). Adeno-associated viral vectors for retinal gene transfer. *Prog. Retinal Eye Res.* **22:** 705–719.
20. Rolling, F. (2004). Recombinant AAV-mediated gene transfer to the retina: gene therapy perspectives. *Gene Ther.* **11**(Suppl. 1)**:** S26–S32.
21. Auricchio, A., *et al.* (2001). Exchange of surface proteins impacts on viral vector cellular specificity and transduction characteristics: the retina as a model. *Hum. Mol. Genet.* **10:** 3075–3081.
22. Rabinowitz, J. E., *et al.* (2002). Cross-packaging of a single adeno-associated virus (AAV) type 2 vector genome into multiple AAV serotypes enables transduction with broad specificity. *J. Virol.* **76:** 791–801.
23. Yang, G. S., *et al.* (2002). Virus-mediated transduction of murine retina with adeno-associated virus: effects of viral capsid and genome size. *J. Virol.* **76:** 7651–7660.
24. Kashani, Z., Chang, B., Hawes, N., Hurd, R., Heckenlively, J. R., and Nusinowitz, S. (2003). Comparison of electroretinographic responses across eleven normal in-bred mouse strains. *Invest. Ophthalmol. Visual Sci. ARVO E-Abstr.* **44:** 1896.
25. Lavallee, C. R., Chalifoux, J. R., Moosally, A. J., and Balkema, G. W. (2003). Elevated free calcium levels in the subretinal space elevate the absolute dark-adapted threshold in hypopigmented mice. *J. Neurophysiol.* **90:** 3654–3662.
26. Behn, D., *et al.* (2003). Dark adaptation is faster in pigmented than albino rats. *Doc. Ophthalmol.* **106:** 153–159.
27. Wu, J., Peachey, N. S., and Marmorstein, A. D. (2004). Light-evoked responses of the mouse retinal pigment epithelium. *J. Neurophysiol.* **91:** 1134–1142.
28. Auricchio, A., Hildinger, M., O'Connor, E., Gao, G. P., and Wilson, J. M. (2001). Isolation of highly infectious and pure adeno-associated virus type 2 vectors with a single-step gravity-flow column. *Hum. Gene Ther.* **12:** 71–76.
29. Liang, F. Q., Anand, V., Maguire, A., and Bennett, J. (2000). Intraocular delivery of recombinant virus. *Methods Mol. Med.* **47:** 125–139.
30. Tavella, S. (1997). Regulated expression of fibronectin, laminin and related integrin receptors during the early chondrocyte differentiation. *J. Cell Sci.* **110**(Pt 18)**:** 2261–2270.